Applied Physics A (2020) 126:689
https://doi.org/10.1007/s00339-020-03879-7

Applied Physics A
Materials Science & Processing

Second harmonic generation and spectroscopic characteristics of TiO_2 doped Li_2O–Al_2O_3–B_2O_3 glass matrix

A. Prabhakar Reddy[1] · Puli Nageswar Rao[2] · M. Chandra Shekhar Reddy[3] · B. Appa Rao[4] · N. Veeraiah[5]

Received: 21 May 2020 / Accepted: 3 August 2020
© Springer-Verlag GmbH Germany, part of Springer Nature 2020

Abstract
In this present study, Li_2O–Al_2O_3–B_2O_3 glass matrix doped with a small percentage of TiO_2 (ranging from 0 to 1 mol%) was prepared and characterized by X-Ray Diffraction (XRD), FTIR and Differential Scanning Calorimetric (DSC) techniques. After that, Optical Absorption (OA), Photo Luminescence (PL), Electron Paramagnetic Resonance (EPR) and Second Harmonic Generation (SHG) have been performed as a function of TiO_2 concentration. The outcome of these studies spelled out different oxidation states of Ti ions. However, sample containing up to about 0.8 mol% of the TiO_2, mostly will be in the state of Ti^{4+} with substitutional octahedral arrangement in the glass chain and is responsible for PL. Beyond this percentage, it is noticed that some parts of Ti ions reduced Ti^{4+} to Ti^{3+} state. The results of Photo-Induced Second Harmonic Generation (PSHG) together with other spectroscopic studies were discussed for all chosen samples and indicated that the Photo-Induced Birefringence (PIB) of sample with 0.8 mol% TiO_2 is the most suitable for NLO (non-linear optics) devices.

Keywords Differential scanning calorimetry · Optical absorption · Photo-induced second harmonic generation · Non-linear optical studies

1 Introduction

Optically poled oxide glasses are selected because of their wide use in optoelectronics on account of their outstanding optical characteristics. The stability of electrical field generated within this type of glasses is a vital issue for deciding the higher harmonic generations within the glass materials.

Normally, TiO_2 is used as crystallizing agent [1] in glass materials like borate glasses; however, by adding small quantity of titanium oxide, the chemical durability and the glass forming ability of the glasses are enhanced [2]. In the glass matrices, generally the Ti ions are found in Ti^{4+} state and participate with TiO_4, TiO_6 and also TiO_5 (having trigonal bipyramids) structural units [3, 4]. However, there are reports revealing that these ions may also exist in the state of Ti^{3+} [5, 6] in some of the glass networks. In alkali oxyborate glasses, the Ti^{4+} ions are better to produce non-linear optical properties to the larger amount because of unfilled orbitals and lower bond lengths [7], as reported bond length between Ti–O is 1.96 Å [8]. The TiO_2 glasses exhibit non-linear negative refractive index that generates a radiation beam of self-focusing in the material; hence non-linear optical (NLO) devices with such chemical compounds are operated at a less significant input power [9, 10].

Addition of Al_2O_3 into the glass, cross-links the neighboring chains of the borate with its structural units of AlO_4; hence, the chemical strength of these glasses is assumed to be enhanced. Further, aluminum oxide increases the T_g (glass transition temperature), reduces the coefficient of thermal expansion, there by makes these glasses more difficult to be attacked by ions of alkali metals like Na^+, Li^+ and so forth [11]. Li_2O is known to be a traditional modifier oxide, which penetrates into the glass network by disrupting cross connections. Normally, the oxygen ion particles crack the

✉ Puli Nageswar Rao
nageswarapuli@gmail.com

1 Department of H&S, Sreyas Institute of Engineering and Technology, Hyderabad 500068, India

2 Department of S&H, St. Martin's Engineering College, Secendrabad 500100, India

3 Department of H&S, CMR College of Engineering and Technology, Medchal 501401, India

4 Department of Physics, Osmania University, Hyderabad 500007, India

5 Department of Physics, Acharya Nagarjuna University, Nagarjunanagar, Guntur 522510, A.P., India

Published online: 10 August 2020

local symmetry and the interstitial positions occupied by Li ions [12].

In the present study, $Li_2O-Al_2O_3-B_2O_3$ glasses were prepared with varying concentrations of TiO_2 and characterized by various techniques viz., X-ray diffraction, DSC, FTIR, EPR, photo luminescence, photo-induced changes and the obtained results were correlated with the variations in the glass structure.

2 Materials and methods (Experimental)

For the present study, the molar compositions of the glasses $30Li_2O-(5\text{-}x)Al_2O_3-65B_2O_3:xTiO_2$($x=0$, 0.2, 0.4, 0.6, 0.8 and 1.0) are chosen and labeled as AT0, AT2, AT4, AT6, AT8 and AT10, respectively. Details of AT system are given below:

AT0: $30\ Li_2O-5Al_2O_3-65B_2O_3$:0 TiO_2.
AT2: $30\ Li_2O-4.8Al_2O_3-65B_2O_3$:0.2 TiO_2.
AT4: $30\ Li_2O-4.6Al_2O_3-65B_2O_3$:0.4$TiO_2$.
AT6: $30\ Li_2O-4.4Al_2O_3-65B_2O_3$:0.6$TiO_2$.
AT8: $30\ Li_2O-4.8Al_2O_3-65B_2O_3$:0.2$TiO_2$.
AT10: $30\ Li_2O-4\ Al_2O_3-65B_2O_3$:1$TiO_2$.

All above glasses were prepared by melt-quenching procedure with high-quality reagents of Li_2CO_3, Al_2O_3, H_3BO_3 and titanium oxide (rutile, tetragonal form) powders in suitable quantities (all in mol%) and were weighed, after that, altogether blended in an agate mortar and dissolved in a crucible of platinum within the range of temperature 1000–1050 ℃ in an electrical furnace for around 30 min, the bubble-free melt formed is poured into a brass mould and annealed subsequently at 300 ℃ for 2 h. The obtained TiO_2-doped glass samples were mechanically ground and polished. Then, the obtained samples were made around 1 cm × 1 cm × 0.2 cm dimensions and OA is taken. For XRD, FTIR, DSC, EPR and PISH studies, the obtained glasses were made into fine powders using pestle and mortar.

To evaluate the densities according to Archimedes' principle, the samples' masses were estimated with an error of 0.1 mg utilizing Ohaus AR2140 balance digital model. From the measured estimations of the samples density and average molecular weight M_w, other different physical parameters, i.e., molar volume V_m (Avg. molecular weight/Density), oxygen packing density O (Oxygen mol percentage × 100/Molar volume), N_i concentration of titanium ion particles ((Avagadro number x mol concentration x valence of ion)/molar volume), mean titanium particles ion separation R_i ($1/N_i^{1/3}$), polaron radius Rp($(\pi/12*(N_i)^{1/3})$, Field strength F_i)(Z/r_p^2), in glass samples are assessed using standard equations [14] and utilizing the refractive index, other different optical parameters viz., molar refraction (R_m), electronic polarizability (α_e) have also been computed [13, 15–17]

The XRD of all the prepared AT samples was recorded on mini flex Rigaku diffractometer with Cu–K_α radiation. DSC of all the prepared AT samples was carried out by Netzsch, simultaneous DSC/TG thermal analyzer STA409C with 32-bit controller. The FTIR transmission spectra of AT samples were recorded in the spectral range 400–1600 cm^{-1}using Perkin Elmer Spectrometer. Using JASCO Model V-670 UV–VIS–NIR spectrophotometer, the optical absorption (OA) spectra in the spectral wavelength range from 300 to 700 nm of the AT samples were recorded at room temperature. The excitation, decay and emission measurements of TiO2 doped samples were recorded on a Jobin–Yvon Fluorolog-3 spectrofluorimeter; xenon arc lamp (450 W) was used as an excited source. Electron spin resonance (EPR) spectra of all AT powder samples were recorded using X-Band JEOL JESTE 100 spectrometer in 8.8–9.6 GHz frequency range at room temperature.

3 Results and discussion

From the measured estimations of the all AT samples' density, average molecular weight M_w and different other physical parameters are presented in Table 1. The molar volume of the glass pattern seems to be increased, whereas the oxygen packing density is reduced with the proportional raise of titanium ion (Ti^{4+}) concentration (Fig. 1). Such a decrease indicates a corresponding decrease in the structural compactness of the samples [18, 19].

The X-ray difractograms of AT0 to AT10 samples are presented in Fig. 2 and the non-appearance of sharp crests in the pattern of diffraction indicates the samples' amorphous nature.

In Fig. 3, differential scanning calorimetric (DSC) graph is presented for different concentrations of TiO_2-doped $Li_2O–Al_2O_3–B_2O_3$ glasses recorded in the region of temperature range of 300–1100 K. The information with DSC studies (from Fig. 3) is given in Table 2. All these DSC traces exhibited conventional glass T_g (glass transition temperature) with the inflection values between 634 and 734 K succeeded by an exothermic peak T_c (crystallization peak temperature) in the temperature range 880 − 930 K and also succeeded another endothermic peak about 1100 K because of melting effect T_m (melting temperature). Although these inflection points corresponding to weak endothermic of all the samples are almost similar, it is interesting to note that values of Tg (glass transition temperature) display an oscillating behavior with increase in the percentage of the TiO_2. For the most part, the changes in the density of expanded cross-link of different structural gatherings and closeness of packing are responsible of such variety of Tg parameter. Thermal analysis of the samples suggests that the AT8 sample has low glass transition temperature T_g indicating higher

Table 1 Physical parameters of $Li_2O-Al_2O_3-B_2O_3$ glasses doped with titanium ions

Name of the sample	AT0	AT2	AT4	AT6	AT8	AT10
Average MW,M(g/mol) = Total MW/100	59.3	59.26	59.21	59.17	59.13	59.08
Density ρ (gcm^{-3}) (+0.001)	1.858	1.821	1.792	1.765	1.729	1.692
Molar volume V_m (MW/ρ) (+0.01)	31.92	32.54	33.04	33.52	34.2	34.92
Oxygen mole %	2.400	2.398	2.396	2.394	2.392	2.390
Oxygen packing density, O (gm atom/L) (+0.01)	75.19	73.69	72.52	71.42	69.94	68.44
Ti^{+4} ion concentration, $N_i(\times 10^{21}/cc)$ (+0.01)	0.00	0.15	0.29	0.43	0.56	0.69
Inter ionic distance, $R_i(A^O)$ (+0.01)	0.00	18.82	15.11	13.25	12.13	11.32
Refractive Index, *n* (+0.01)	2.19	2.20	2.23	2.28	2.34	2.29
Molar refraction, R_M(+0.01)	17.83	18.27	18.82	19.55	20.48	20.46
Polarizability $(\alpha_e)(\times 10^{-24})$ (cm^3)(+0.01)	7.07	7.25	7.46	7.75	8.12	8.11
Polaranradious (R_p) (A^0)	0.00	0.76	0.61	0.53	0.49	0.46
Field strength F_i (10^{16})	0.00	6.93	10.75	14.24	16.66	18.9

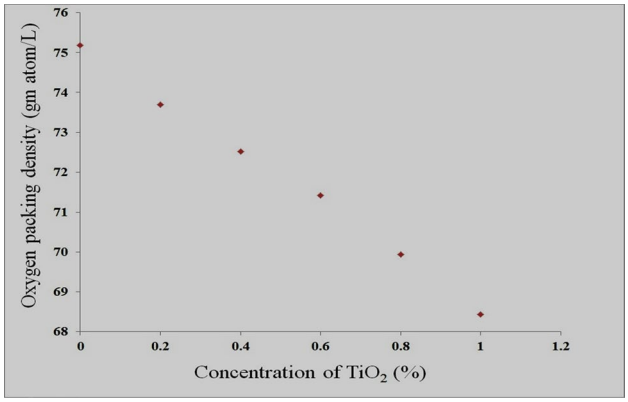

Fig. 1 Variation of oxygen packing density of Li_2O-Al_2O_3–B_2O_3:TiO_2 glasses

structural disorder in this sample. The expansion in estimation of enthalpy with increment of dopant till 0.8 mol% indicates where crystallization begins at first inside the glass and extends to the surface bit by bit [20–25].

The spectra of infrared transmission of the Li_2O–Al_2O_3–B_2O_3 glasses containing different concentrations of TiO_2 recorded at room temperature are shown in Fig. 4. The band positions and their functional groups of $Li_2O-Al_2O_3-B_2O_3$:TiO_2 glasses are shown in Table 3. The initial array of bands in the regions 1200 to 1600 cm^{-1} is because of B–O bond expanding relaxation of the trigonal BO_3 units, while the second array of bands at 900–1050 cm^{-1} referred to units of BO_4 and the band appearing at 698 cm^{-1} is due to the vibrations of bending modes of B–O–B links in the network of borate [18, 19]. The bond at 698 cm^{-1} could also be the vibrational band appearing at about 698 cm^{-1} in the glass network in fact may also represent the vibrations of TiO_4 groups as reported in the literature [20]. Hence, the bond at 698 cm^{-1} could be referred to common vibrations of TiO_4 groups of linkages of B–O–Ti in the same region

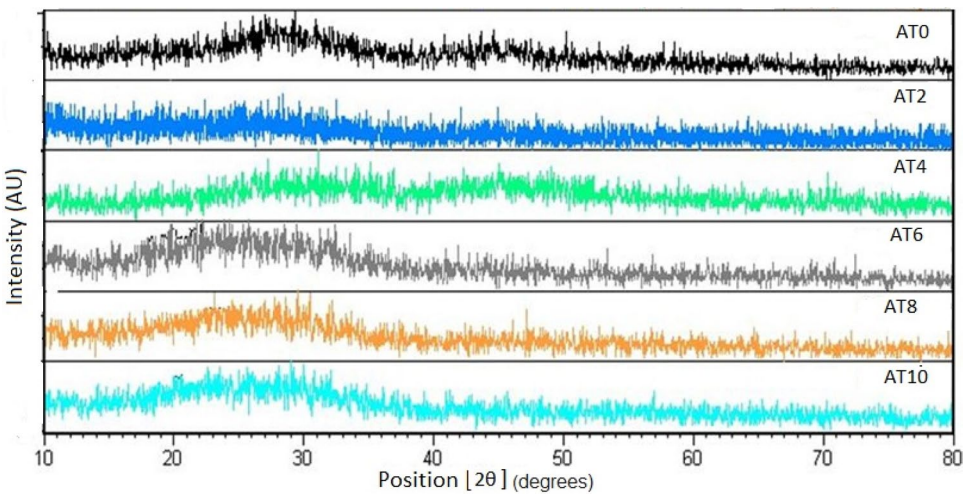

Fig. 2 X- ray diffraction Patterns of Li_2O–Al_2O_3–B_2O_3 glasses doped with titanium ions

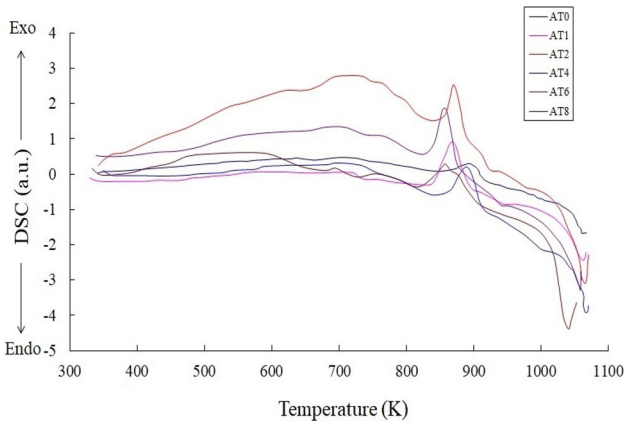

Fig. 3 DSC traces of Li_2O–Al_2O_3–B_2O_3:TiO_2 glasses

[21]. Tangentially, AlO_4 structural units also exhibit a band with the vibrational frequency of Al–O stretching and form linkages of B–O–Al.

As per FTIR spectra, with the presence of titanium oxide up to 0.8 mol% in glass network, the magnitude of vibrational band due to BO_4 groups is noticed to decrease with the moving of meta-center (1050 cm^{-1}) towards higher wave number (1076 cm^{-1}), whereas for BO_3 group, it is seen to increase with the moving of meta-center (1508 cm^{-1}) towards low wave number (1481 cm^{-1}) as shown in Table 3. In both the cases, when concentration of TiO_2 is more than 0.8 mol%, the variation of intensity with the TiO_2 concentration displayed a reverse pattern. Furthermore, all the glasses displayed functional groups at 691 cm^{-1}. While concentration of TiO_2 in the glass framework is raised up to 0.8 mol%, the position of the common metacentre of B–O–Ti is seen to move towards higher frequency with diminishing intensity. These perceptions recommend that the system of glass AT2 (shown in Fig. 3) has higher grouping of linkages of kind B–O–Ti and is highly rigid while the disorderness in the glass system continues increasing with that of TiO_2 concentration upto 0.8 mol%. It is currently sure that titanium ion exists in both Ti^{4+} (arranged in both tetrahedral and

Table 2 Summary of the data on differential scanning calorimetric studies of Li_2O-Al_2O_3-B_2O_3:TiO_2 glasses

Sample	T_g(K)	T_c(K)	T_m(K)	T_c-T_g(K)	T_m-T_c(K)	T_c-T_g/T_m-T_c	ΔH(J/g)	ΔC_p(J/g K)
AT0	634.4	921	1100	286.6	179	1.601	191.3	0.229
AT2	739.6	892	1100	152.4	208	0.732	208.4	0.986
AT4	739.8	912	1120	172.2	208	0.827	219.6	1.509
AT6	738.0	888	1100	152.0	212	0.707	295.0	1.512
AT8	634.3	888	1100	253.7	212	1.196	295.7	1.529
AT10	734.4	893	1100	154.6	207	0.746	276.8	1.198

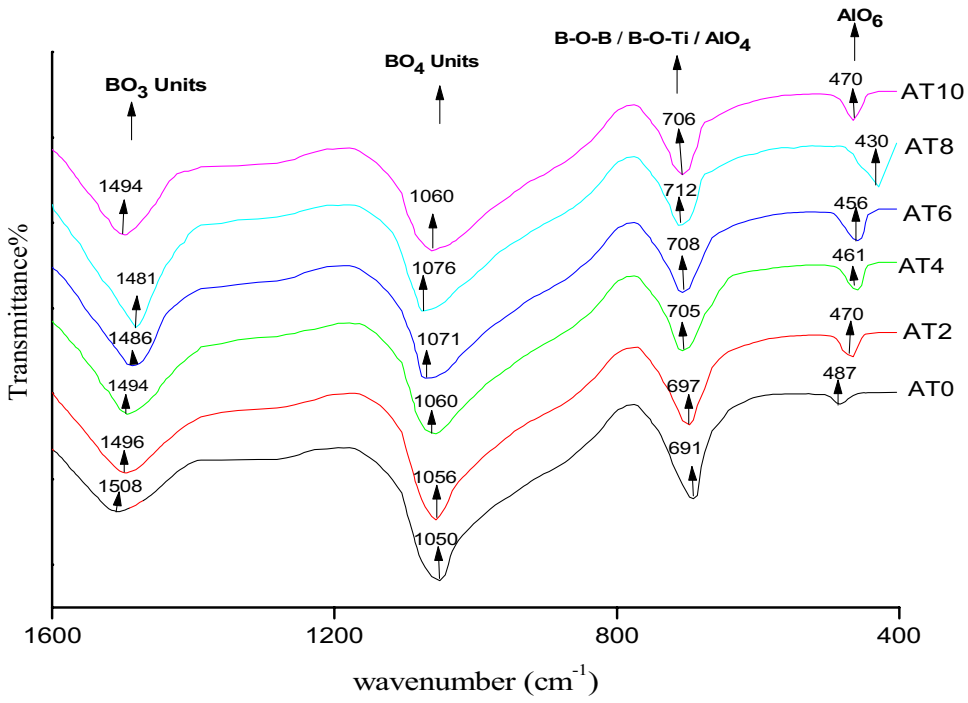

Fig. 4 FTIR Spectra of Li_2O–Al_2O_3–B_2O_3 glasses doped with TiO_2

Table 3 The observed band positions and their assignments of Li_2O-Al_2O_3-B_2O_3:TiO_2 glasses

Glass	BO_3groups (cm^{-1})	BO_4 groups (cm^{-1})	B–O–B/B–O–Ti/ AlO_4 (cm^{-1})	AlO_6 (cm^{-1})
AT0	1508	1050	691	487
AT2	1496	1056	697	470
AT4	1494	1060	705	461
AT6	1486	1071	708	456
AT8	1481	1076	712	430
AT10	1494	1060	706	470

Table 4 Optical absorption spectra information on Li_2O-Al_2O_3-B_2O_3:TiO_2 glasses

Sample	Cut-off wavelength in nm	$^2B_{2g} \rightarrow {}^2B_{1g}$ nm	$^2B_{2g} \rightarrow {}^2A_{1g}$ Nm	Optical band-gap in eV
ATO	309.68	–	–	3.89
AT2	334.95	496	660	3.84
AT4	339.11	501	662	3.72
AT6	346.32	505	663	3.49
AT8	349.08	504	660	3.24
AT10	349.92	508	664	3.44

octahedral positions) and in Ti^{3+} (situated octahedral sites) states in these glasses. Further, the spectra of all the glasses displayed a band around 487 cm^{-1} which might be expected due to AlO_6 units [26]. The intensity of vibrational band due to these units increased with the increase in the concentration of titanium oxide up to 0.8 mol% and the meta-center switched towards lesser wavelength side, and for further increase of TiO_2 concentration, it is decreased.

Spectra of optical absorption of titanium oxide-doped alumina borate glasses recorded in the wavelength region around 300–700 nm are shown in the Fig. 5. Appropriate information identified with the optical retention spectra of all the glass samples is given in Table 4.

Two distinct bands of absorptions observed in the optical absorption spectra of AT2 to AT10 at 500 and 660 nm are distinguished as being because of $2B_{2g} \rightarrow 2B_{1g}$ and $2B_2 \rightarrow 2A_{1g}$ transitions of $3d^1$ electron of the Ti^{3+} ions in distorted tetragonal octahedral positions [27, 28].

With the data collected from absorption spectra, optical band-gap E_o of the sample was calculated. Urbach plots (Fig. 6) are drawn in between $(\alpha hv)^{1/2}$ versus hv according to Eq. (1) and cut-off wavelength, absorption bands,

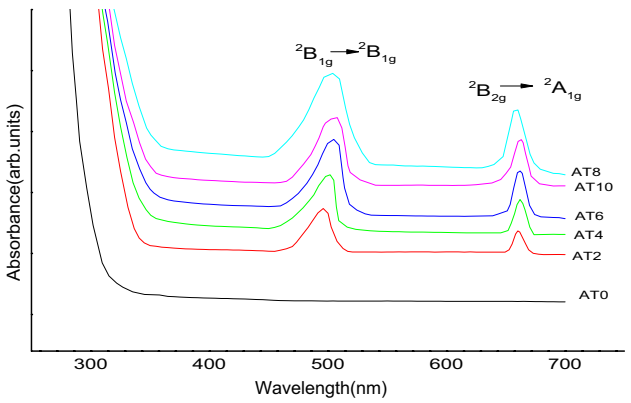

Fig. 5 Optical absorption Spectra of Li_2O–Al_2O_3–B_2O_3:TiO_2 glass system

optical band-gap are given in Table 4. It can be seen that optical band-gap of the sample AT8 has the least value.

$$\alpha(\omega)\hbar\omega = const(\hbar\omega - E_0)^2$$

Here $\alpha(\omega)$ is optical absorption coefficient.

With the increase of content of TiO_2, intensity of two bands and the half width is enhanced, with a move in the positions of band towards higher wavelength regions. The peak intensity of these group bands was recognized in the spectrum of AT8 sample; this observation denotes the maximum concentration of Ti^{3+} ions in this glass matrix. The lesser presence of these bands in the spectrum of the AT2 glass apparently shows the fewer existence of Ti^{3+} ions in this glass.

Luminescence emission spectra of TiO_2-doped Li_2O–Al_2O_3–B_2O_3 glasses recorded at room temperature and excited at wavelength resembling to their absorption edge are shown in Fig. 7. On increasing the concentration of TiO_2 up to 1.0 mol%, the half width of this band and the intensity were also noticed to decrease. The emission spectrum of the AT2 glass sample with peak position at 457 nm is shown.

Applying the general formula [24] for transition probability:

$$A(\psi_j, \psi_{j'}) = \frac{8\nu^2}{e^2} \times 10^6$$

And for cross section of emission,

$$\sigma_P^E = \frac{\lambda^4}{8\pi c n_d^2 \Delta\lambda} A(\psi_j, \psi_{j'})$$

The relevant information identified with emission spectra is presented in Table 5. In Eq. (3),ν is the frequency and c is velocity of the radiation, n_d is the refractive index of the sample; $\Delta\lambda$ represents half width of the peak of the emission. The estimation of σ_P^E is observed to be the highest for the AT2 sample, implying higher glow productivity for this sample.

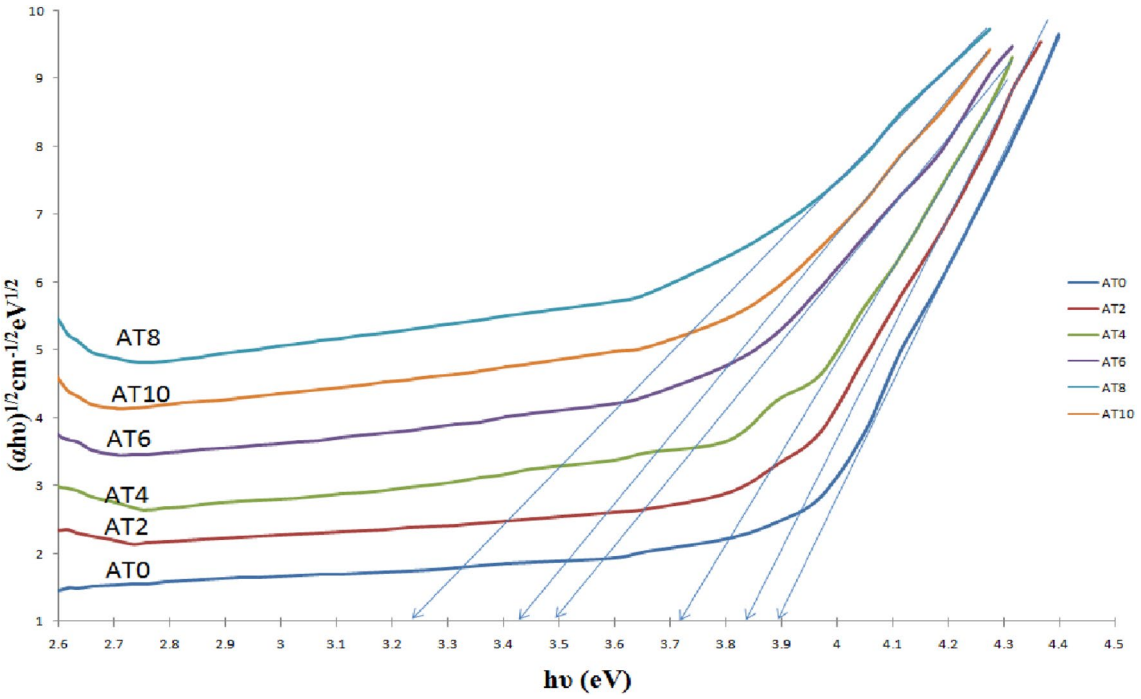

Fig. 6 Urbach plots of Li_2O–Al_2O_3–B_2O_3:TiO_2 glasses

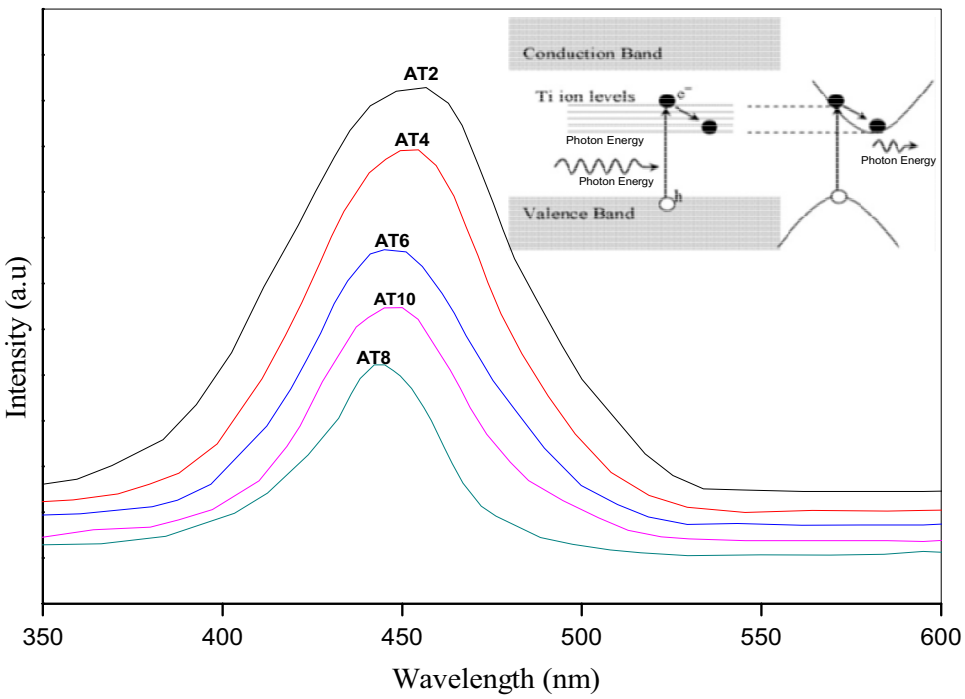

Fig. 7 Luminescence emission spectra of Li_2O–Al_2O_3–B_2O_3:TiO_2 glasses. The inset demonstrate the mechanism for PL emission

Blasse [30] comprehensive study on titanium ion particles containing closed-shell transition metal suggested that titanium ion exhibits luminescence in both octahedral and tetrahedral complexes. However, the luminescence efficiency established by complexes of octahedral substitutionally situated Ti^{4+} particles is a lot more noteworthy than that of tetrahedral complexes. The band of luminescence is referred to radiative recombination of STEs (self trappedexcitons) confined on a substitutionally situated octahedral Ti^{4+}ions. The observed emission band can be explained by credible

Table 5 Emission cross-section (σ_P^E) and transition probability (**A**) of Li_2O-Al_2O_3-B_2O_3 glasses

Glass	Emission peak Position in nm	Refractive index	A ($\times 10^{34}$)	$\sigma_P^E(\times 10^{28},cm^2)$
AT2	457	1.560	1.7749	6.203
AT4	455	1.549	1.7432	5.677
AT6	447	1.548	1.7354	5.447
AT8	442	1.557	1.6603	4.582
AT10	446	1.559	1.6749	4.635

mechanism in elaborated way as pursues. The valence band of this sort of material is ordinarily shaped by 2p orbitals of O^{2-} ions.

These glasses must be containing octahedrally situated substitutional Ti^{4+} ionsalong with $(TiO6)^{8-}$ structural basic units [31]. Charge move from O^{2-} goes into the unfilled 3-d orbital of Ti^{4+} ion making it into Ti^{3+} state. The caught d-electrons when energized make interaction with the lattice vibrations of electron–phonon. The relaxation energy after photo excitation advances the spatial division of pairs of hole–electron demonstrated in inset of the Fig. 7. The samples containing substitutional Ti^{4+} particles with a low concentration in the glass web either a hole or an electron are feebly localized, indicating the concentration of TiO_2 dependence of the luminescence.

EPR spectra of different concentrations of TiO_2–Al_2O_3–B_2O_3 glasses recorded at 26 °C are shown in Fig. 8. The g values for all the samples are shown in Table 6. The AT2 glass shows a asymmetric weak signal with $g = 1.914$ because of $3d^1$ unpaired electron of Ti^{3+} particles in a distorted tetragonal octahedral field [32]. Both the intensity of the signal and the half width of the signal are gradually increasing in the spectra of the glasses with further increase of TiO_2 up to 0.8 mol%, after which it is

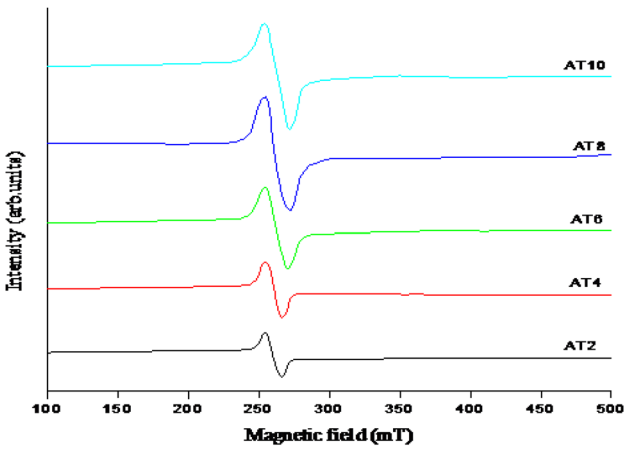

Fig. 8 Spectra of EPR ofLi_2O–Al_2O_3–B_2O_3:TiO_2 glasses

Table 6 g -values of Li_2O-Al_2O_3-B_2O_3:TiO_2 glasses

Glass	*g*- Value
AT2	1.914
AT4	1.925
AT6	1.933
AT8	1.947
AT10	1.938

seen to decrease. It demonstrates an expanding concentration of Ti^{3+} ions in the glass network. The presence of such Ti^{3+} particles weakens the glass network. The weak intensity noted for glass AT2 apparently demonstrates the presence of low concentration of these ions in this glass.

Figure 9 represents the comparison plot of the difference of PIB with the photo-inducing power; it is observed that a generous increment of the PIB output is associated with the increase of the pumping power for total samples. The figure shows a gradual increment of photo-induced birefringence intensity till concentration 0.8 mol% of TiO_2, and for further increase of TiO_2 content, a fast decrease is noticed.

The investigations on PIB showed the highest intensity of birefringence for the AT8 sample; it is conclusive on the grounds that the same AT8 sample is owning minimum optical energy gap. This is very vital in terms of outcome of the present investigation, since it permits to conclude that Ti ions encompassing ligands assume leading role in the noticed PIB. To be specific, more significantly the contribution of the octahedral coordinated Ti^{3+} ions may be noticed. Lastly, the scrutiny of the outcome of PIB combined with collection of other experimental conclusions indicates that among different glass samples, the Li_2O–Al_2O_3–B_2O_3:TiO_2 glass with 0.8 mol % of titanium oxide (TiO_2) is a decent contender for the applications in NLO (nonlinear optics) gadgets.

4 Conclusion

The absence of peaks in XRD reveals all the prepared glass samples are non-crystalline (amorphous) in nature. The results of DSC suggest that the sample AT8 exhibits low T_g value which is suggestive of more disordered structure. The IR spectral studies show that boron, aluminum, and Ti ions take part in the glass web BO_3, BO_4, B–O–B, B–O–Ti, AlO_4, AlO_6 structural units. Further, the outcome also indicates that the concentration of high-order structural units viz., BO_4, AlO_4 (which make the glass network more rigid), are less in the AT8. The OA (optical absorption) and EPR studies of the glass system indicate the presence of the trivalent Ti ions apart from tetravalent state. However, samples containing titanium oxide beyond 0.8 mol% of the Ti occur mostly in the state of Ti^{4+}. Photo luminescence spectra of

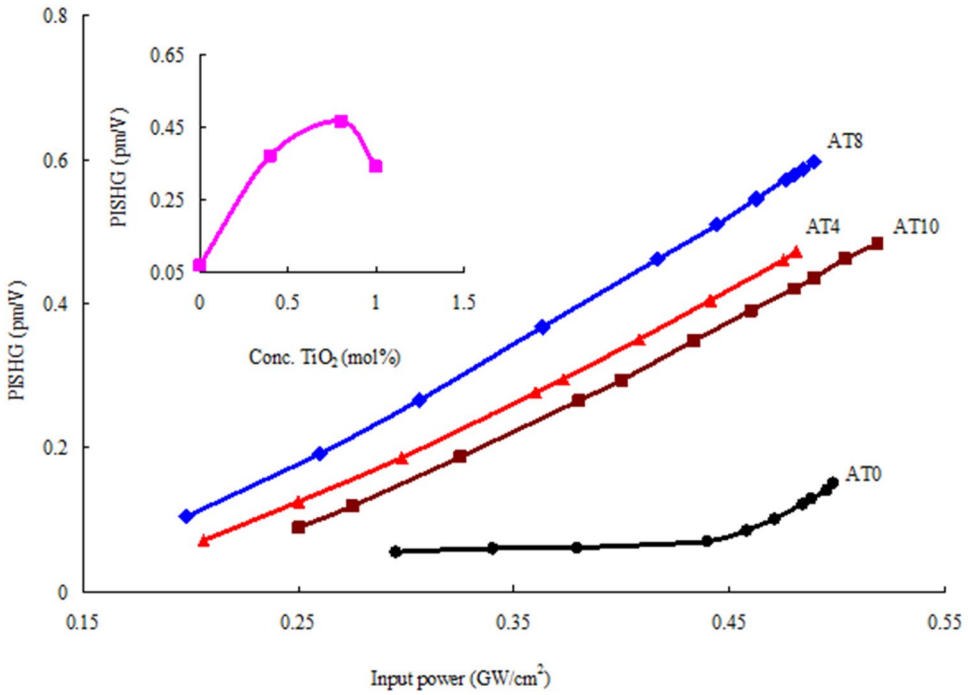

Fig. 9 Comparison plots of the PISHG of Li_2O–Al_2O_3–B_2O_3:TiO_2 glasses

these glasses excited at wavelengths corresponding to their absorption edges exhibit a wide emission band in the visible domain. The agitation of substitutionally octahedral positioned Ti^{4+} ions is noticed to be responsible for the luminescence emission. The investigations on PIB noted a growing intensity of SHG signal with increasing TiO_2 concentration, and this result is correlated with simultaneous red shift in the optical band-gap noticed. This perception permits us to infer that the neighboring ligands of octahedrally placed titanium ions (Ti^{3+}) play vital role in the noticed PISHG.

References

1. M.A. Marzouk, F.H. ElBatal, H.A. ElBatal, TiO2 on the optical, structural and crystallization behavior of barium borate glasses. Optical Materilas **57**(2016), 14–22 (2016). https://doi.org/10.1016/j.optmat.2016.04.002
2. R. Balajirao, D. KrishnaRao, N. Veeraiah, The role of titanium ions on structural, dielectric and optical properties of Li2O–MgO–B2O3 glass system. Mater Chem Phys **87**, 357–369 (2014). https://doi.org/10.1016/j.matchemphys.2004.05.045
3. Prabhakar Reddy A, Chandra Shekhar Reddy M, Siva Sesha Reddy A, Ashok J, Veeraiah N, AppaRao B (2018) Photo-induced non-linear optical studies on gallium alkali borate glasses doped with TiO2, Applied Physics A 124:755. Doi: 10.1007/s00339-018-2178-0
4. M. Nagarjuna, T. Satyanarayana, Y. Gandhi, N. Veeraiah, Influence of Ag2O on some physical properties of LiF–TiO2–P2O5 glass system. J. Alloy. Compd. **479**, 549–556 (2009). https://doi.org/10.1016/j.jallcom.2008.12.132
5. T. Satyanarayana Y, Gandhi M, A Valente, I. V. Kityk, N. Veeraiah, Influence of titanium ions on spectroscopic properties of TeO2–Sb2O3–B2O3: TiO2 glass ceramics, Phys. Status Solids C 8 (2011) 3082–3086, https://doi.org/10.1002/pssc.201000750
6. R.K. Brow, D.R. Tallant, W.L. Warren, A. McIntyre, D.E. Day, Thermal properties and stability of lithium titanophosphate glasses. Phys. Chem. Glasses **38**, 300 (1997). https://doi.org/10.1007/s10973-008-9192-y
7. M. Sahoo, A.K. Yadav, S.N. Jha, D. Bhattacharyya, T. Mathews, N.K. Sahoo, S. Dash, A.K. Tyagi, Nitrogen location and Ti–O bond distances in pristine and N-doped TiO2 anatase thin films by x-ray absorption studies. J. Phys. Chem. C **31**, 17640–17647 (2015). https://doi.org/10.1021/acs.jpcc.5b03295
8. D. Lundberg, I. Persson, Structure of a hydrated sulfonatotitanyl(IV) complex in aqueous solution and the dimethylsulfoxide solvated Titanyl(IV) ion in solution and solid state. J. Solution Chem. **46**, 476–487 (2017). https://doi.org/10.1007/s10953-017-0581-3
9. L.-H. Guo, Y.-W. Wang, Y.-Q. Jiang, S. Xiao, J.H. Chin, Dependence of nonlinear optical response of anatase TiO2 on shape and excitation intensity. Phys. Lett. **34**, 077803 (2017). https://doi.org/10.1088/0256-307X/34/7/077803
10. N. Narasimharao, I.V. Kityk, V. Ravi Kumar, C. Srinivasarao, M. Piasecki, P. Bragiel, N. Veeraiah, Dc field induced optical effects in ZnF2–PbO–TeO2:TiO2 glass ceramics, Ceramics Int 38 (2012) 2551–2562.https://doi.org/10.1016/j.ceramint.2011.11.026
11. M. Srinivasa Reddy, G. Naga Raju, G. Nagarjuna, N. Veeraiah, Structural influence of aluminium, gallium and indium metal oxides by means of dielectric and spectroscopic properties of CaO–Sb2O3–B2O3 glass system,, J. Alloys Compounds 438 (2007) 41–51. https://doi.org/10.1016/j.jallcom.2006.08.054
12. C. SrinvasaRao, T. Srikumar, Y. Gandhi, V. Ravikumar, N. Veeraiah, Dielectric and spectroscopic investigations of lithium aluminium zirconium silicate glasses mixed with TiO2. Philosophical Mag **6**, 958–980 (2011). https://doi.org/10.1080/14786435.2010.531056
13. M. Chandra Shekhar Reddy, E. Ramesh Kumar, B. Appa Rao, Optical & ESR studies of lead antimony borate glasses doped with V2O5. Int. J. Sci. Eng. Res. **5**, 3 (2014)

14. M.J. Weber, R. Cropp, J. Non-Cryst, Solids **4**, 137 (1981)
15. H.A. Lorentz, Ann. Phys **9**, 641 (1980)
16. M Chandra Shekhar Reddy, A. Prabhakar Reddy, K Krishnamurthy Goud, B. Appa Rao, Physical and optical properties of PbO–Sb2O3–B2O3 Glasses Doped with Gd2O3, Materials Todays 3 (2016) 3970–3975 https://doi.org/10.1016/j.matpr.2016.11.058
17. V. Dimitrov, T. Komatsu, an interpretation of optical properties of oxides and oxide glasses in terms of the electronic ion polarizability and average single bond strength. J Univ Chem Technol Metallurgy **45**, 219 (2010)
18. S. Cetinkaya Colak, Role of titanium ions on the optical and thermal properties of zinc borate glass doped with TiO2. Phys. Chem. Glasses **58**, 41–48 (2017). https://doi.org/10.13036/17533562.57.2.067
19. M.R. Reddy, S.B. Raju, N. Veeraiah, Optical absorption and fluorescence spectral studies of Ho3+ ions in PbO–Al2O3–B2O3 glass system. J. Phys. Chem. Solids **61**, 1567 (2000). https://doi.org/10.1016/S0022-3697(00)00035-4
20. PuliNageswarRao, E. Ramesh Kumar, M. Chandra Shekhar Reddy, A. Prabhakar Reddy, K. Krishnamurthy Goud and B. Appa Rao (2018), Optical studies of AgI–Ag2SO4–TeO2–B2O3 glass system, Materials Today 5(13), Part 1, 2018, 26329-26338. https://doi.org/10.1016/j.matpr.2018.08.084
21. P.N. Rao, E. Ramesh Kumar, B. Appa Rao, Structural and transport studies of CdI2-doped silver boro tellurite fast ion-conducting system. J. Solid State Electrochem. **22**, 3863–3871 (2018). https://doi.org/10.1007/s10008-018-4094-9
22. M. Manickam, P. Singh, T.B. Issa et al., Electrochemical behavior of anatase TiO2 in aqueous lithium hydroxide electrolyte. J ApplElectrochem **36**, 599–602 (2006). https://doi.org/10.1007/s10800-005-9112-9
23. P. NageswaraRao, D. KrishnaRao, N. Veeraiah, Indian J. Eng. Mater. Sci. **13**, 69–74 (2006)
24. M. Kumar, A. Uniyal, A.P.S. Chauhan, S.P. Singh, Optical absorption and fluorescent behaviour of titanium ions in silicate glasses. Bull. Mater. Sci. **26**, 335–341 (2003). https://doi.org/10.1007/BF02707456
25. F. Branda, A. Buri, A. Marotta, S. Saiello, Kinetics of crystal growth in Na2O_2SiO2 glass A DTA study. Thermochim Acta **77**, 13–18 (1984)
26. Y. Gandhi, M. V. Ramachandra Rao, C. Srinvasa Rao, T. Srikumar, I. V. Kityk, N. Veeraiah, Influence of aluminum ions on fluorescent spectra and upconversion in codoped CaF2–Al2O3—P2O5–SiO2:Ho3+ and Er3+ glass, J. Appl. Phys. 108, 023102 (2010). https://doi.org/10.1063/1.3464257
27. N. Shimoji, T. Hashimoto, H. Nasu, K. Kamiya, Non-linear optical properties of Li2O–TiO2–P2O5 glasses. J. Non-Cryst. Solids **324**, 50–57 (2003). https://doi.org/10.1016/S0022-3093(03)00178-9
28. X Zhu, Q Li, N Ming, Z Meng., Origin of optical nonlinearity for PbO, TiO2, K2O, and SiO2 optical glasses, Appl. Phys. Lett. 1997, 71:867. https://doi.org/10.1063/1.119672
29. A. Aboukais, L.D. Bogomolova, A.A. Deshkovskaya, V.A. Jachkin, N.A. KrasilNikova, S.V. Stefanovsky, E.A. Zhilinskaya, EPR of silica and fluoride glasses implanted with titanium and zirconium. Opt Mater **19**, 295–306 (2002). https://doi.org/10.1016/S0925-3467(01)00226-9
30. G. Murali Krishna, Y. Gandhi, N. Veeraiah, Luminescence spectroscopy of Ti ions in Li2O–CaF2–P2O5 glass ceramics. J. Luminescence **128**, 631–634 (2008). https://doi.org/10.1016/j.jlumin.2007.10.034
31. M. Watanabe, T. Hayashi, Time-resolved study of self-trapped exciton luminescence in anatase TiO2 under two-photon excitation. J. Lumin. **112**, 88 (2005). https://doi.org/10.1016/j.jlumin.2004.09.001
32. L.D. Bogomolova, N.A. Krasilnikova, S.A. Prushinsky, O.A. Trul, S.V. Stefanovsky, J. Non-Cryst, Solids **292**, 59 (2001)

Publisher's Note Springer Nature remains neutral with regard to jurisdictional claims in published maps and institutional affiliations.